JOURNAL OF MATERIALS SCIENCE 27 (1992) 557–568

# Thermal, structural and textural studies on the double complex salt $[Co(NH_3)_6][Fe(CN)_6]$ and on its silica-supported catalysts

L. H. KHALIL*, N. A. MOUSSSA
*Department of Chemistry, Faculty of Science, Ain Shams University, Cairo, Egypt*
S. MIKHAIL
*Egyptian Petroleum Research Institute, Nasr City, Cairo, Egypt*

Thermal analyses were carried out for the simple complexes $[Co(NH_3)_6]Cl_3$ and $K_3[Fe(CN)_6]$ together with the double complex $[Co(NH_3)_6][Fe(CN)_6]$ using thermogravimetric analysis, differential thermal analysis (DTA) and derived DTA (DDTA). Two series of silica-supported catalyst samples were prepared with soaking periods ranging from 5 h to 7 days, and likewise investigated. Structural changes of the original samples and their thermally treated products obtained at temperatures $< 500\,^{\circ}C$ were monitored using X-ray diffraction and infrared spectroscopy.Textural variations were also studied using the $N_2$ adsorption technique. The decomposition of the simple complex $[Co(NH_3)_6]Cl_3$ occurs in two main steps that give rise to two asymmetric endothermic peaks centred at 225 and 350 °C. The first step involves two decomposition processes in which primarily two chloride ions migrate to the inner coordination sphere, thereby releasing two coordinated $NH_3$ that are evolved, followed by simultaneous decomposition and reduction to $CoCl_2 \cdot 2NH_3$. The second step involves the decomposition of this latter compound to $CoCl_2$ with some reduction to Co. $K_3[Fe(CN)_6]$ decomposes in a more complex manner, yet two strong exotherms are observed at ~345 and 400 °C – the former being accompanied by a loss in weight due to its decomposition, whereas the latter is accompanied by a small increase in weight where an oxidation process seems to take place with its further decomposition. The double complex $[Co(NH_3)_6][Fe(CN)_6]$ exhibits five consecutive decomposition steps in the temperature range 210–305 °C. The first is reproduced as an endotherm at ~180 °C, whereas the remaining four steps cannot be distinguished separately by DTA due to the strong exothermic effects and only two exotherms are observed at ~255 and 280 °C. The steps are identified according to the simultaneous reaction of six molecules together, leaving a final solid product with empirical formula $Fe(CN)_2Co$. X-ray diffraction of the double complex retains the characteristics of the constituent simple complexes with the appearance of two new very strong bands with a *d*-spacing of 0.5483 and 0.3005 nm. The specific surface areas of the catalyst samples are found to depend on the ion moiety supported first during preparation as well as on the soaking period. The catalyst samples are predominantly microporous and the variations in surface characteristics are discussed. $V_l$–$t$ plots reveal the presence of two groups of pore sizes in some cases.

## 1. Introduction

The preparation and study of double complexes is becoming a major interest of research to explore the metal–metal interactions [1–3]. Special attention is paid to their dependence on the nature of the bridging group in the binuclear complexes that play a significant role in the M–L–M′ bond angle [4].

Thermal dehydration and thermal reactions are widely applied to prepare cyano-bridged binuclear cobalt complexes, focusing attention on the thermal bridging reaction by which metal–metal interactions occur [5–11]. However, the reaction schemes and products are found to vary widely with the experimental conditions [8, 10].

Since the transition metals are the ones which are of greatest importance as catalysts [12], a postulated and interesting application would be the preparation of such complexes on a suitable support in an attempt to ultimately prepare supported dispersed metallic (or metal-oxide) catalysts in which the two metals (or their oxides) are always the same distance apart over the entire support surface. If the control of such

---

*To whom correspondence should be addressed.

0022–2461/92 $03.00 + .12

metal–metal distances is achieved, it may open a new approach to catalyst preparations.

In the present study, the double complex $[Co(NH_3)_6][Fe(CN)_6]$ was investigated using thermogravimetric analysis (TGA), differential thermal analysis (DTA), derived DTA (DDTA), X-ray diffraction and i.r. Also, a series of catalyst samples was prepared using silica as support. The catalyst samples were also investigated by the above techniques together with the study of their texture using $N_2$ adsorption at 77 K.

## 2. Experimental procedure

### 2.1. Materials

### *2.1.1. Simple complexes*

$[Co(NH_3)_6]Cl_3$ was prepared by the method reported in the literature [13] using reagents of AR grade. It was identified by means of elemental analysis and spectrophotometric measurements. The $K_3[Fe(CN)_6]$ complex was a Merck AR product.

### *2.1.2. Double complex*

200 ml of 0.05 M solution of $[Co(NH_3)_6]Cl_3$ were added gradually with constant stirring to 200 ml of a 0.05 M solution of potassium ferricyanide where immediate and complete precipitation was observed. The product was allowed to stand for about 6 h to ensure complete precipitation. The precipitate thus obtained was filtered, washed several times with distilled water, ethanol and ether, then air-dried. The colour of the double complex was brownish orange. It should be noted that the double complex $[Co(NH_3)_6][Fe(CN)_6]$ is very sparingly soluble and could not be recrystallized from water or any other solvent. Therefore, the starting materials used in the preparation of the double complex were of the AR grade.

The analysis of the double complex gave 5.20% H, 20.08% C and 44.95% N in accordance with the calculated values.

### 2.2. Catalyst samples

The silica used as support for the preparation of the catalyst samples was a product for chromatography (BDH). The surface characteristics of this silica, as obtained from $N_2$ adsorption, indicate it to be predominantly microporous with a specific area ($S_{BET}$) of $\sim 344\ m^2\,g^{-1}$ and a total pore volume, $V_{P0.95}$, of 0.2044 ml (taken as a liquid volume at $P/P_0 = 0.95$) and average pore radius, $r_H$, of 1.18 nm ($r_H = V_{P0.95}/S_{BET}$). Two series of samples were prepared by precipitating the double complex on the surface, depending on which simple complex was added first to the silica. Thus, 30 ml of a 0.05 M solution of $K_3[Fe\ (CN)_6]$ was added to 30 g silica with thorough stirring. The mixture was left for the desired period of time, then filtered and washed once with 10 ml distilled water and refiltered. To this product 30 ml of a 0.05 M solution of $[Co(NH_3)_6]Cl_3$ complex was added, aiming at its reaction with the already adsorbed ferricyanide complex anion moiety. The product was left for the same time interval as that previously used for the first simple complex, filtered and washed once as before and then left to dry at room temperature.

This product supplied the samples for series I in which the iron complex was added first. The same procedure was repeated but with $[Co(NH_3)_6]Cl_3$ added first to the silica gel; then the $K_3[Fe(CN)_6]$ solution was added, giving rise to series II. The soaking periods for these two series of samples were 5 h and 2, 5 and 7 days. Thermal decomposition products were obtained by heating all samples in the presence of air for 2 h at 250 and 450 °C, except those soaked for 5 days. The product used will be denoted by its sample symbol (I or II) with the subscript indicating the soaking period, and the treatment temperature (°C) noted for samples heated at 250 and 450 °C.

### 2.3. Techniques

Thermal analysis was carried out in the presence of static air by a simultaneous TGA and DTA apparatus using a Netzsch Gerätebau GmbH, Selb apparatus (Type No. 348 472C) at a heating rate of $5\ ^\circ C\,min^{-1}$. The inert reference used was α-alumina for DTA.

X-ray diffraction patterns were obtained by a Philips diffractometer unit, Model pM 9920/03, using Fe-filtered Co-radiation. The *d* spacings were calculated and their relative intensities compared with data in the ASTM cards [14, 15].

I.R. spectra of the samples were measured with a Pye-Unicam SP3-200A spectrograph using KBr pellets.

Adsorption–desorption isotherms of nitrogen at 77 K were determined by a conventional volumetric gas adsorption apparatus.

## 3. Results and discussion

### 3.1. Thermal and structural characteristics

TGA of the simple cobalt ammine complex $[Co(NH_3)_6]Cl_3$ over the temperature range ambient to 500 °C is characterized by two main decomposition steps. The first step commences above 100 °C, showing a slow decomposition stage up to ~ 290 °C that is followed by an abrupt loss in weight up to ~ 302 °C (Fig. 1a). In this step, two stages of decomposition seem to occur consecutively. The first stage covers a wide temperature range, namely 100–290 °C, and appears to take place as a result of the migration of two chloride ions to the inner coordination sphere [16] to occupy the sites of two coordinated ammonias that are released in the process according to the equation

$$[Co(NH_3)_6]Cl_3 \rightarrow [Co(NH_3)_4Cl_2]Cl + 2NH_3\uparrow \qquad 12.74\%$$

This is immediately followed by another decomposition process that is accompanied by a further ~ 26% loss according to the equation

$$[Co(NH_3)_4]Cl_2]Cl \rightarrow [CoCl_2 \cdot 2NH_3] + \text{volatile product} \qquad 25.98\%$$

The presence of ammonia in the product so obtained was confirmed by testing with hot concentrated sodium hydroxide solution.

The reduction of $Co^{3+}$ to $Co^{2+}$ probably takes place in an early stage of the decomposition, similarly to other systems in which a change of valency to lower oxidation states was observed [11, 17]. The X-ray pattern obtained for a sample heated at 250 °C for 1 h (Fig. 2a) is found to be completely different from that reported for the parent material or that of the final product $CoCl_2$ [14, 15] (see Fig. 2b). It is quite probable that this points to a product with the formula $[CoCl_2 \cdot 2NH_3]$.

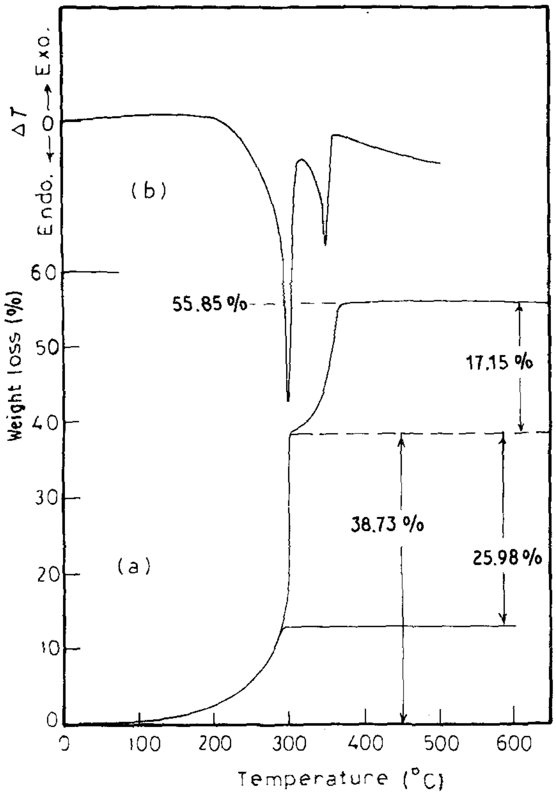

*Figure 1* (a) Thermogravimetric and (b) differential thermal analysis curves for $[Co(NH_3)_6]Cl_3$.

The second decomposition step follows immediately after the first step and terminates at ~ 375 °C, giving a total percentage loss of 55.85. In this last step, if the loss is referred to the initial weight of the material, a value of 17.15% loss is obtained that fits well with the following postulated decomposition process:

$$6[CoCl_2 \cdot 2NH_3] \rightarrow 5CoCl_2 + Co + \text{volatile products} \quad 17.15\%$$

It is worth noting that the X-ray pattern of a sample heated at 340 °C for 1 h is identified to be $CoCl_2$ (Fig. 2b). The volatile products resulting from the previous two reactions may be $NH_3$, $Cl_2$, $NH_4Cl$ or $N_2$, bearing in mind that $NH_3$ can behave as a reducing agent.

The experimental percentage loss of each stage, as obtained by TGA (referring to the initial weight of starting material) is found to fit very well with the corresponding theoretical value calculated according to the predicted stage given above. However, it is well known that thermal decomposition of coordinated compounds is quite sensitive to the surrounding atmosphere.

Simultaneous DTA results lead to the same speculations as before (Fig. 1b). Thus, two main endothermic

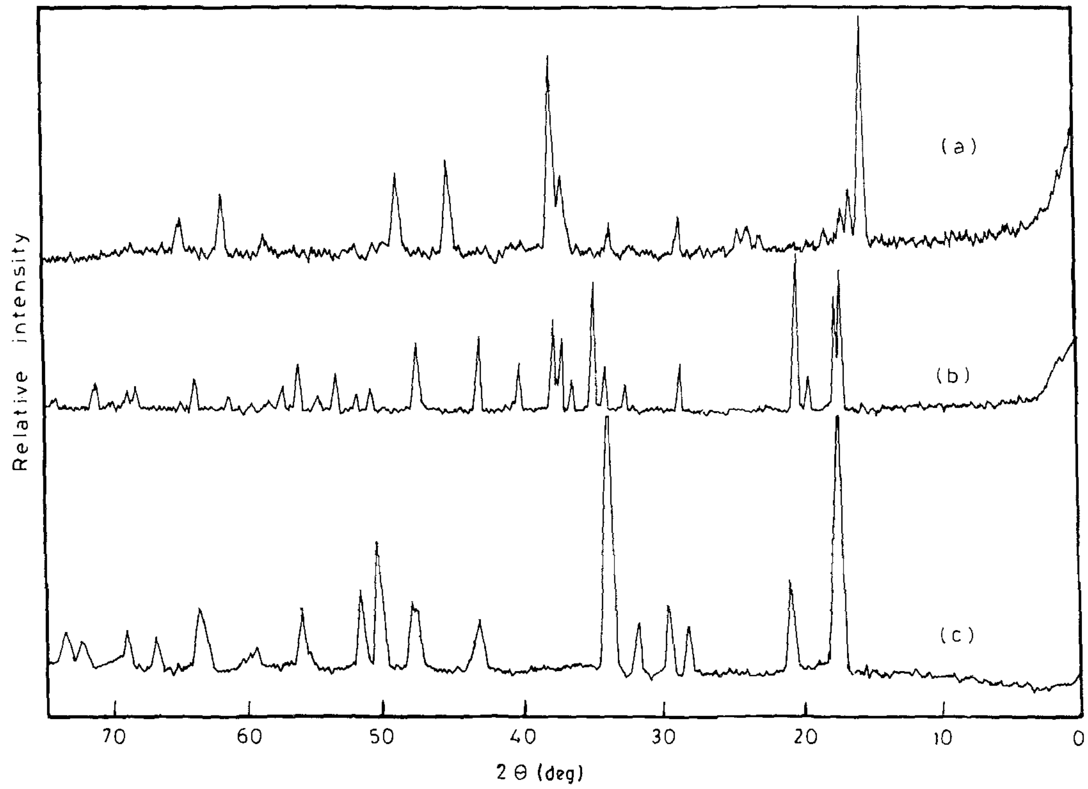

*Figure 2* X-ray diffraction patterns for (a) $[Co(NH_3)_6]Cl_3$ heated 250 °C, 1 h; (b) $[Co(NH_3)_6]Cl_3$ heated 340 °C, 1 h; (c) the double complex salt $[Co(NH_3)_6][Fe(CN)_6]$.

peaks are observed centred at 295 and 350 °C that correspond to the two major decomposition stages, each preceded by a wider endothermic effect that is also reflected in the DDTA curves (not shown here), i.e. the peaks are not symmetrical. In the case of the first endotherm, the peak covers the two decomposition stages of the first step observed in TGA, where the commencement of the endotherm reflects the evaluation of the two $NH_3$ molecules (~12.74%). The reduction of $Co^{3+}$ to $Co^{2+}$ in this stage should also produce an endothermic effect that seems to coincide with that resulting from the $NH_3$ evolution in the second stage (~26%), thus giving rise to only one very strong endothermic peak.

The second endotherm appears as a result of the decomposition of the product $[CoCl_2 \cdot 2NH_3]$ to $CoCl_2$ and Co, in which two processes are actually taking place simultaneously: the evolution of $NH_3$ and the reduction of $Co^{2+}$ to Co. Since the reduction is probably conducted by the evolved ammonia, it seems reasonable to believe that it is the $NH_3$ that is evolved first in the temperature range 320–350 °C, followed by the reduction of some $Co^{2+}$ to Co. This is reflected in the shape of the endotherm centred at ~ 350 °C, which exhibits a much wider area at the lower-temperature side of the peak than at the higher-temperature side. Reduction to metallic cobalt was previously reported to occur at higher temperatures [18].

TGA of $K_3[Fe(CN)_6]$ shows a gradual small initial weight loss up to ~ 300 °C of about 1.98%, followed by a slightly larger weight loss up to ~ 350 °C above which an increase in weight is observed (Fig. 3a). Simultaneous DTA shows a small shift of the base line with the ultimate formation of a very small broad endotherm centred at 244 °C that appears to correspond to the initial gradual weight loss (Fig. 3b). This may result from the evolution of some trapped water within the crystal framework that is evolved prior to its rupture.

The larger weight loss observed at higher temperatures in the TGA curves is accompanied by a very strong exothermic effect centred at ~345 °C. Above this temperature, another strong exotherm is observed centred at ~400 °C that is accompanied by an increase in weight. This exotherm seems to result from an oxidation process, probably accompanied by the evolution of cyanogen and the conversion of the iron to the oxide form upon decomposition of the complex. An overlap in the resulting changes in weight makes the complete analysis at this stage difficult. This complexity was also observed by Duval [19].

TGA of the solid double complex $[Co(NH_3)_6][Fe(CN)_6]$ shows five distinct steps covering the temperature range 125–310 °C (Fig. 4a). These steps could be identified on the basis of six molecules reacting simultaneously. Taking into consideration the decomposition of each simple complex alone, it is convenient to believe that the ammonia should be evolved first. Table I gives the termination temperature of each step, the species believed to be detached from the solid and the experimental percentage loss. The theoretical percentage loss (column 5) is found to conform very well with the experimental data (column 4) for each evolved species. From this table, most of the ammonia is first evolved alone (first and second steps) and then the $(CN^-)$ species commences to be evolved. The final solid is then left with the 12(CN) for 6Co and 6Fe (or 2CN:1Co:1Fe). It is worth emphasizing that though the TGA curve exhibits clearly the various steps, one

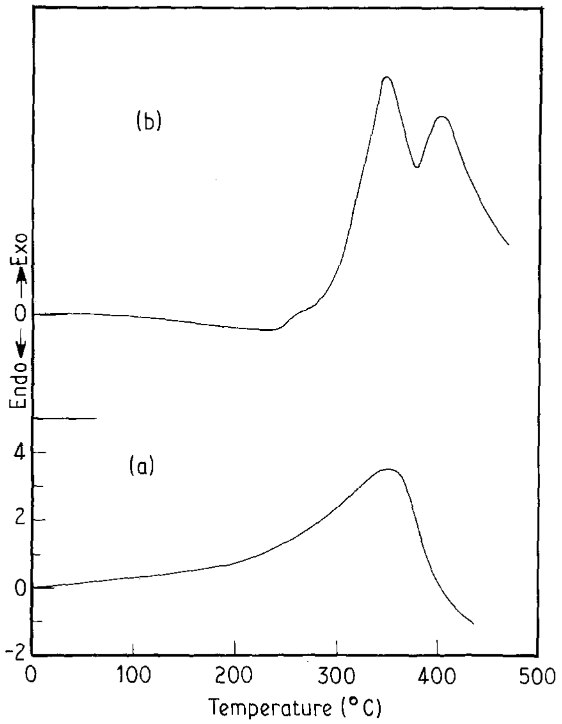

*Figure 3* (a) Thermogravimetric and (b) differential thermal analysis curves of $K_3[Fe(CN)_6]$.

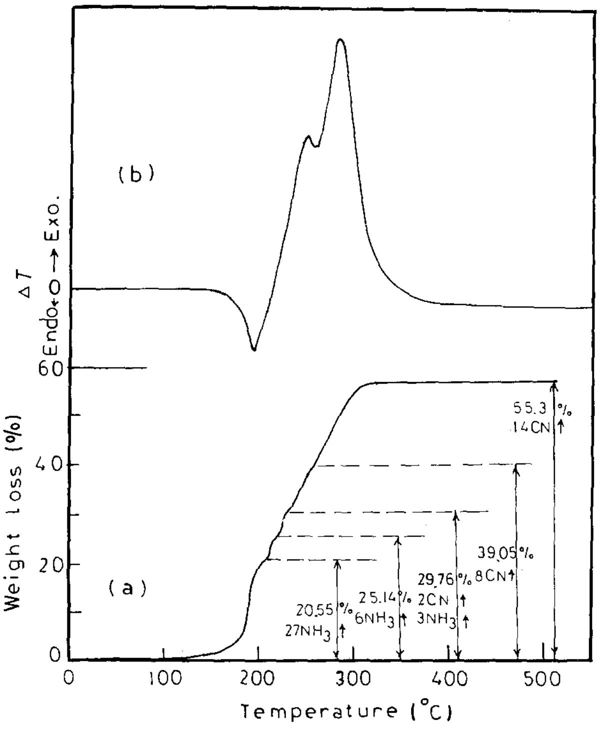

*Figure 4* (a) Thermogravimetric and (b) differential thermal analysis curves of the double complex salt $[Co(NH_3)_6][Fe(CN)_6]$.

TABLE I Percentage losses and corresponding detached species encountered upon heating the double complex salt

| Step | Temperature (°C) | Species abstracted from solid | Experimental loss (%) | Theoretical loss (%) |
|---|---|---|---|---|
| First | 210 | $-27NH_3$ | 20.55 | 20.54 |
| Second | 222 | $-6NH_3$<br>$-3NH_3$ | 25.14 | 25.11 |
| Third | 235 | $-2CN$ | 29.76 | 29.71 |
| Fourth | 262 | $-8CN$ | 39.05 | 39.01 |
| Fifth | 306 | $-14CN$ | 55.30 | 55.28 |

could not possibly obtain a solid sample that comprises the composition of a single stage as the decompositions follow each other immediately without exhibiting any constant state over a controlled temperature range, and any sample obtained will be contaminated with other product constituents.

Thus, the first decomposition step resulting from the evolution of $NH_3$ is reproduced as an endotherm at ~190 °C in the DTA curve (Fig. 4b). The four remaining decomposition steps are not reproduced separately as a result of the strong exothermic effects resulting from the decomposition processes and removal of the ($CN^-$), and only two exotherms are observed at ~255 and ~280 °C.

Decomposition of a similar complex in the presence of argon gas gave only one exotherm and a different reaction path was postulated [11], thus emphasizing the role of the surrounding atmosphere and experimental conditions on the reaction mechanism and consequently on the resulting decomposition products.

Infrared spectral analysis curves obtained before and after heating the double complex salt to 300 °C for 1 h show that the CN vibrational bands (2120 and 2080 $cm^{-1}$) are reduced but still exist (Fig. 5, curve d). These are compared with that obtained for pure unheated $K_3[Fe(CN)_6]$ (Fig. 5, curve a). However, it is noted that the intensity of the band at 2120 $cm^{-1}$ is markedly reduced for the heated product but it did not disappear. Chemical analysis of this heated product showed the presence of some excess of nitrogen over that of the predicted ratio of Co:2CN:Fe and a very little percentage of $H_2$. This is clearly understood from differences in the experimental conditions of TGA and heating in an electric oven, where overlap of the decomposition stages and/or readsorption of the evolved gases upon cooling can give such deviations.

It is noticed that though the simple complex $K_3[Fe(CN)_6]$ shows an oxidation process (increase in weight) at temperatures > 350 °C, yet in the double complex salt no such increase is observed. Moreover, the decomposition of the double complex salt is complete at temperature $\leqslant 310$ °C as also found for similar systems [10], whereas that of each simple complex alone exceeded 350 °C so that a lowering in decomposition temperature is achieved. A small band observed at ~800 $cm^{-1}$ characterizes a Co–N vibration [20], showing the cobalt to be attached to the nitrogen of the CN group.

X-ray analysis curves of the original double complex retained the characteristic bands of each simple complex alone, beside the appearance of two new very

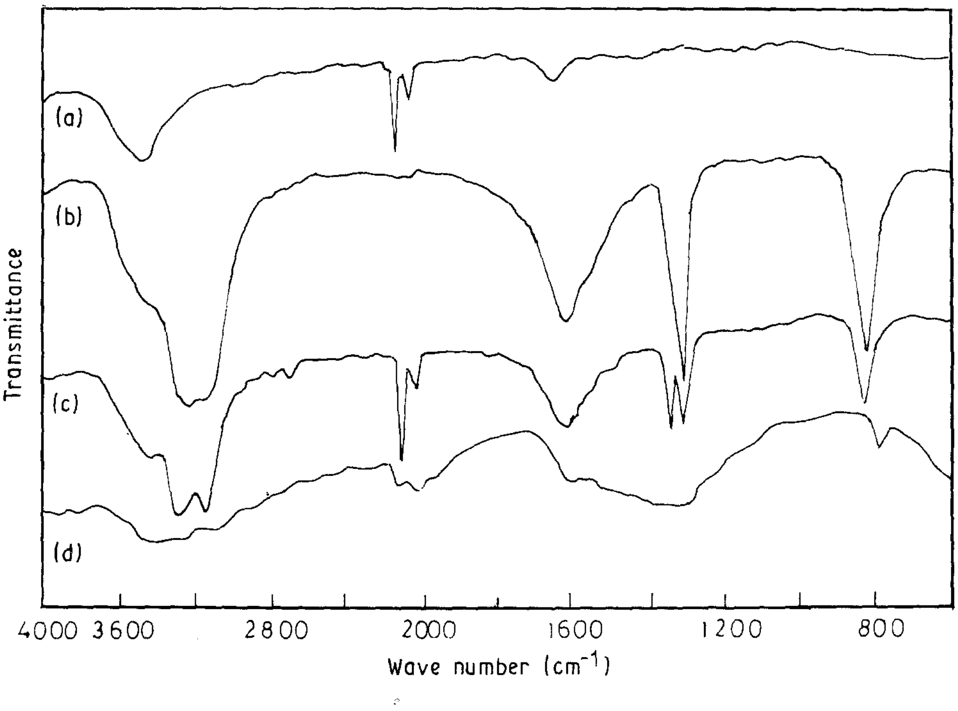

*Figure 5* Infrared spectra of (a) $K_3[Fe(CN)_6]$, (b) $[Co(NH_3)_6]Cl_3$, (c) $[Co(NH_3)_6][Fe(CN)_6]$, (d) the double complex heated at 300 °C for 1 h.

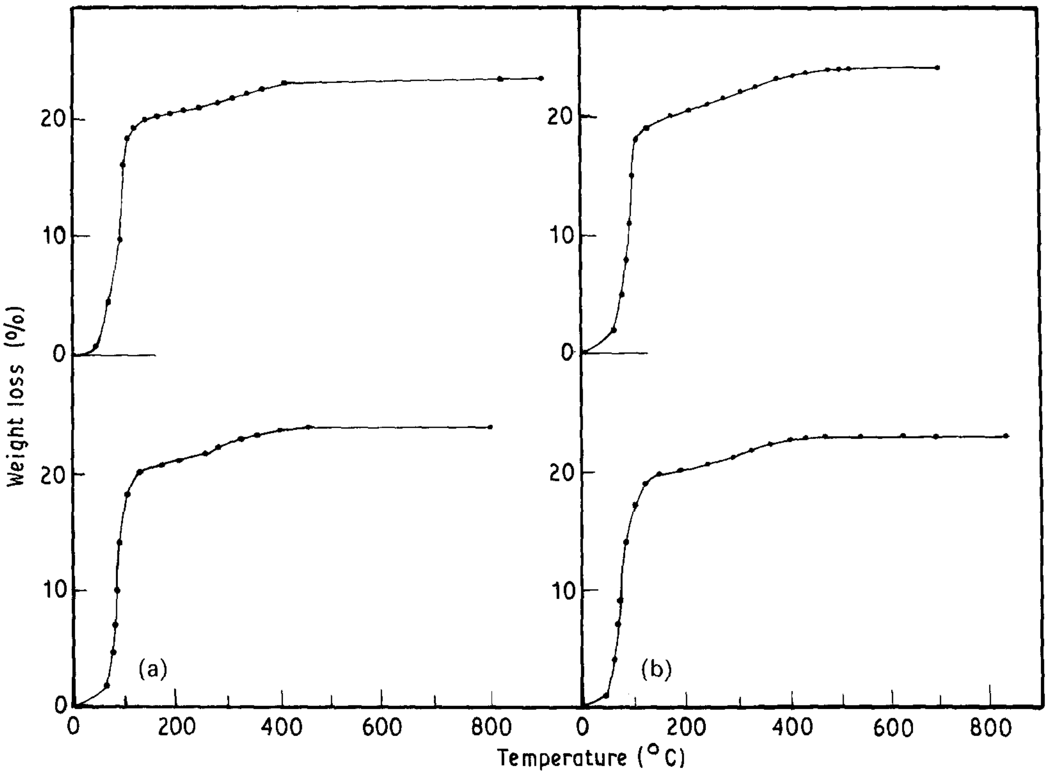

*Figure 6* TGA curves of catalyst samples from (a) series I and (b) series II soaked for 5 h and 7 days.

strong bands at 2θ values of 18.8 and 34.7 ° (*d*-spacings 0.5483 and 0.3005 nm, respectively) (Fig. 2c). It appears that this new double complex, though combining the structures of both simple complexes, yet exhibits the above two characteristic bands because the extremely strong electrostatic attraction present between the complexes brings them together, close enough to approach bond distances. The double complex would then be expected to undergo thermal changes that are somewhat different from its individual components, as actually observed above.

TGA curves of the supported catalyst samples show an initial weight loss in the temperature range 50–150 °C and amounting to about 20%. This arises from the dehydration of silica, being the same for all the catalyst samples. Above 150 °C, another gradual decomposition stage is observed that covers the temperature range up to ~ 450 °C. The loss of this step is found to vary with soaking period, being a maximum for the sample soaked for 7 days. It arises from the decomposition of the complex as well as from dehydration of the silica. Fig. 6 shows the TGA curves for samples from series I and II soaked for 5 h and 7 days. Samples soaked for 7 days give the same total percentage loss, pointing to the presence of nearly equal amounts of supported complex irrespective of the nature of the initially absorbed ion moiety.

## 3.2. Surface characterization of the catalyst samples

Full adsorption–desorption cycles of nitrogen were obtained for all the original catalyst samples soaked for the various periods of time, as well as for those heated at 250 and 450 °C for 2 h for those soaked for 5 h, 2 days and 7 days.

The specific area of the pure double complex is found to be less than 1 $m^2 g^{-1}$; the area measured by the available volumetric technique will be subject to a large error.

### 3.2.1. Effect of type of ion moiety initially supported on silica

The nitrogen isotherms produced for the original samples from series I possess a shape between type I and type II. Thermal treatent at 250 °C does not affect the shape of the sample soaked for 5 h, but that soaked for 2 days shows a nearly linear region of increased adsorption in the relative pressure range from 0.05 to 0.4 followed by a plateau, whereas that soaked for 7 days gives a type II adsorption isotherm. Samples heated at 450 °C exhibit a nearly linear portion up to relative pressures $< 0.4$ irrespective of soaking period.

When the cobalt ammine complex is initially used for the formation of the double complex on the silica, as for series II, the $N_2$ adsorption isotherms are found to exhibit a linear portion in the low-pressure range for all samples except that soaked for 5 days, where a continuous increase in adsorption is observed up to relative pressure 0.6 followed by a plateau. Soaking for 7 days causes a shift of this linear portion to very low pressures, signifying strong adsorption at the initial adsorption stages. Heating the samples at 250 or 450 °C does not much affect the shape of the isotherms; nevertheless, they adopt a shape between type II and I retaining the overall micropore characteristics. In all the samples investigated no hysteresis

TABLE II Surface characteristics of samples of series I and their thermally heated products obtained from nitrogen adsorption

| Sample | BET $C$ constant | $S_{BET}$ ($m^2 g^{-1}$) | $S_t$ ($m^2 g^{-1}$) | $V_{P0.95}$ ($ml g^{-1}$) | $r_H$ (nm) | $m_f$ (%) |
|---|---|---|---|---|---|---|
| $I_{5h}$ | 49 | 430.0 | 422.0 | 0.237 | 1.00 | 52.0 |
| $I_{2d}$ | 157 | 548.0 | 550.0 | 0.287 | 1.04 | 51.3 |
| $I_{5d}$ | 83 | 217.0 | 215.0 | 0.159 | 1.40 | 18.2 |
| $I_{7d}$ | 38 | 455.5 | 470.0 | 0.226 | 1.00 | 50.3 |
| $I_{5h}$-250 | 16 | 584.0 | 566.0 | 0.278 | 0.95 | 43.5 |
| $I_{2d}$-250 | 68 | 428.5 | 430.0 | 0.256 | 1.20 | 59.7 |
| $I_{7d}$-250 | 101 | 430.5 | 427.0 | 0.356 | 1.60 | 39.6 |
| $I_{5h}$-450 | 50 | 288.0 | 288.0 | 0.198 | 1.37 | 48.4 |
| $I_{2d}$-450 | 77 | 376.5 | 368.0 | 0.209 | 1.11 | 55.9 |
| $I_{7d}$-450 | 61 | 271.0 | 270.0 | 0.159 | 1.11 | 52.9 |

TABLE III Surface characteristics of samples of series II and their thermally heated products obtained from nitrogen adsorption

| Sample | BET $C$ constant | $S_{BET}$ ($m^2 g^{-1}$) | $S_t$ ($m^2 g^{-1}$) | $V_{P0.95}$ ($ml g^{-1}$) | $r_H$ (nm) | $m_f$ (%) |
|---|---|---|---|---|---|---|
| $II_{5h}$ | 63.7 | 588.0 | 434.0 | 0.236 | 0.80 | 50.0 |
| $II_{2d}$ | 126.0 | 345.0 | 340.0 | 0.226 | 1.30 | 49.3 |
| $II_{5d}$ | 22.75 | 478.0 | 474.0 | 0.211 | 0.88 | 46.7 |
| $II_{7d}$ | 104.2 | 418.5 | 418.0 | 0.245 | 1.17 | 57.0 |
| $II_{5h}$-250 | 72 | 401.0 | 402.0 | 0.237 | 1.18 | 46.7 |
| $II_{2d}$-250 | > 1000 | 290.0 | 290.0 | 0.211 | 1.46 | 50.7 |
| $II_{7d}$-250 | 98.8 | 268.5 | 280.0 | 0.249 | 1.86 | 39.2 |
| $II_{5h}$-450 | 69.4 | 420.0 | 420.0 | 0.240 | 1.14 | 49.6 |
| $II_{2d}$-450 | 139.0 | 313.0 | 315.0 | 0.249 | 1.60 | 40.0 |
| $II_{7d}$-450 | 70.6 | 285.0 | 268.0 | 0.186 | 1.30 | 46.5 |

phenomenon could be detected, emphasizing the pore size range to be within that which does not permit capillary condensation to take place. Also, the absence of a horizontal plateau extending to near-saturation pressure excludes the formation of a unimolecular layer only, and the adsorption in general seems to be finite with limited pore dimensions. For a reasonable assessment [21] of the fraction of microporosity in the samples, the volume adsorbed at $P/P_0 = 0.05$ is divided by the total pore volume at $P/P_0 = 0.95$, $V_{P0.95}$ (as condensation between particles may occur at relative pressures $> 0.95$). At such a low relative pressure as 0.05 (taken arbitrarily), filling of the pores is more likely to occur where it just exceeds the Henry's law range [22]. Tables II and III (column 7) show these fractions as a percentage (denoted by $m_f$). The specific surface area ($S_{BET}$) is estimated by using the BET equation over its normal range of applicability and taking the molecular area of adsorbed nitrogen as $1.62 \text{ nm}^2$. Application of the Langmuir or Kaganer [23] equations to the adsorption data failed, thereby emphasizing that multilayer adsorption occurred on the samples investigated. The BET $C$ constants, specific surface areas and the total pore volumes are given in Tables II and II (columns 2, 3 and 5, respectively).

The variation of specific area with soaking period is found to depend on which ion moiety is first supported on the silica. This is expected to be so, since the double complex is formed from the anion moiety of one $[Fe(CN)_6]^{3-}$ and the cation moiety of the other $[Co(NH_3)_6]^{3+}$, and therefore the initial attack on the silica surface should, in fact, be different. Thus, when the double complex is formed on a silica surface with the anion moiety applied first (series I), the specific surface area is found to increase upon increasing the soaking period from 5 h to 2 days. This is accompanied by an increase in total pore volume with the value of $m_f$ remaining constant. Such a situation would result from the deeper penetration of the complex inside the pores over the period of 2 days. Though this process is not accompanied by clear changes in the porosity $m_f$, yet the increase in both $V_{P0.95}$ and $S_{BET}$ clearly show that the relatively strong electrostatic forces arising from the initial anion moiety seem, when given enough soaking time, to penetrate through some narrow orifices that become enlarged, thus permitting more space to be measured. This might appear ridiculous, but there actually seems to be a clear change in the morphology of the surface texture as a result of incoming electrostatic and dispersion forces imposed on some specific sites on the silica surface.

When the soaking period is extended to 5 days, an agglomeration process seems to take place, resulting in a decrease in all the surface parameters including $m_f$. In this sample the isotherm has actually changed to type II, emphasizing a type of sintering to have taken place, or that the double complex has blocked most of the very narrow pores, thereby decreasing the area to less than half the value for the sample with a soaking period of 5 h, with a corresponding decrease in $V_{P0.95}$. However, such a situation is not the end of the process and if the soaking period is further extended to 7 days, the complex penetrates deeper into the pores and the pore characteristics approach those obtained for samples soaked for 5 h except that the

BET C constant is markedly decreased (Table II, column 2), pointing to a change in the chemical nature of the surface.

When the supported double complex is precipitated on the silica surface with the cation moiety $[Co(NH_3)_6]^{3+}$ supported first, a different trend is observed. The specific area is found to decrease with soaking period up to 2 days with the total pore volume also slightly decreasing, pointing to the blocking of some of the narrower pores. Increasing the soaking period to 5 days causes an increase in specific area that is not accompanied by a corresponding increase in $V_{P0.5}$ but rather a small decrease is observed (Table III). This implies the generation of some narrow pores formed at the expense of the larger ones upon the penetration and formation of the double complex inside these narrower pores. This is reflected in the $m_f$ value that exhibits a decrease which signifies the size of the pores formed to be that corresponding to relative pressures $> 0.05$.

After 7 days soaking, the solid structure seems to "relax" and overcome the stage of a "strained structure" resulting from the 5 days soaking, and the wide pores seem to become wider at the expense of narrower ones, thereby revealing a group of very narrow pores as reflected by the increase in the $m_f$ value. Such a situation is a result of the changes arising between the dispersion and electrostatic forces of the double complex and the walls of the solid support.

From the above results, it is clear that not only is the type of moiety (cation or anion) significant in the precipitation of a double complex on a support, but also the soaking period markedly affects the surface texture. A period exceeding 7 days may even be necessary for the attainment of maximum surface modification.

### 3.2.2. Effect of thermal treatment

The variation of specific surface area and total pore volume with treatment temperature is found to depend on the initially adsorbed ion moiety. Thus, for

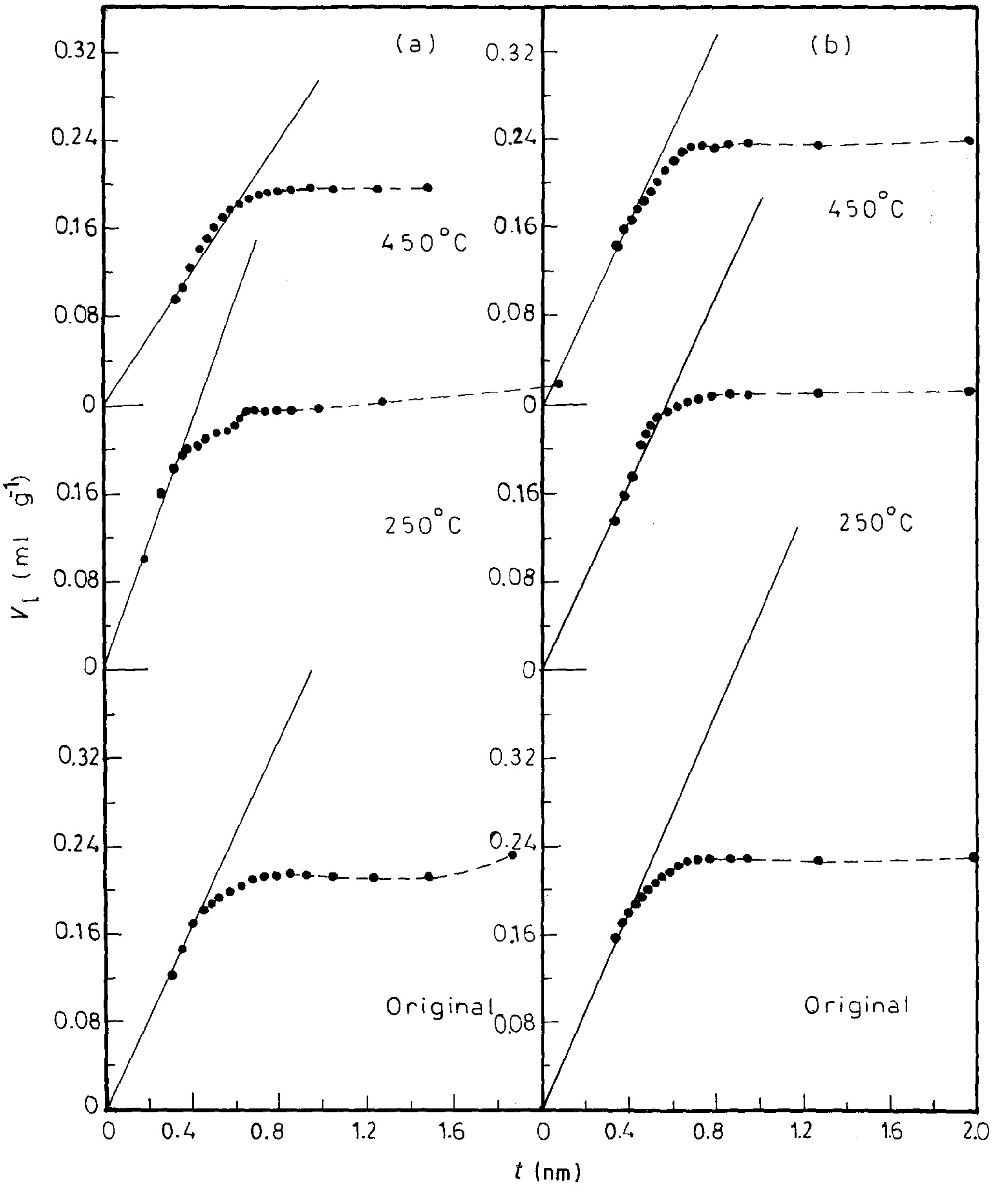

*Figure 7* $V_l$–$t$ plots of samples soaked for 5 h from (a) series I and (b) series II, together with their heated products.

samples of series I, heating the 5 h soaked sample to 250 °C markedly increased the specific surface area, whereas a decrease was observed for the other two samples soaked for 2 and 7 days (Table II, column 3) that give nearly identical results. In this temperature range, most of the double complex is decomposed but the differences in texture observed depend on its location within the pore structure. This is clear for the sample soaked for 7 days where the complex is believed to have the maximum penetration among the series. Though the specific area has slightly decreased, yet the total pore volume has increased, whereas the microporosity, $m_f$, has decreased (columns 5 and 7). This could only result from the evolution of the decomposition products of the double complex as well as the dehydration of the silica structural framework.

At 450 °C, all the specific areas decrease with a collapse or shrinkage of the pore structure, resulting in a decrease in the total pore volume. This is marked for the sample soaked for 7 days where microporosity increased again.

It is worth noting that the variation of the texture of the silica support upon thermal treatment interferes with that resulting from the complex, and we believe that the contribution may be significant for the sample soaked for 5 h, but less so for that soaked for 7 days where the complex is believed to have penetrated deeper into the pore space.

As for the samples of series II, a decrease in specific area is observed by heating to 250 °C, accompanied by negligible changes in the pore volume for all the samples. Further heating to 450 °C produced only a small increase in specific area but the changes imposed on the total pore volumes varied with soaking period. A small decrease in microporosity, $m_f$, is also observed as compared to the original samples.

### 3.2.3. *Pore analysis*

The pore system is identified by using the *t*-method of de Boer *et al.* [24, 25]. The $S_t$ values obtained show fair agreement with the corresponding $S_{BET}$ values, thus indicating a suitable choice of *t* curves [24–28] on the basis of the BET *C* constant (Tables II and III).

The $V_l$–$t$ plots obtained for samples from both series (I and II) are shown in Figs 7–10 for soaking periods from 5 h to 7 days, together with the heated products for samples from 5 h, 2 and 7 days soaking. From these plots, it seems that the samples are predominantly microporous as observed by the down-

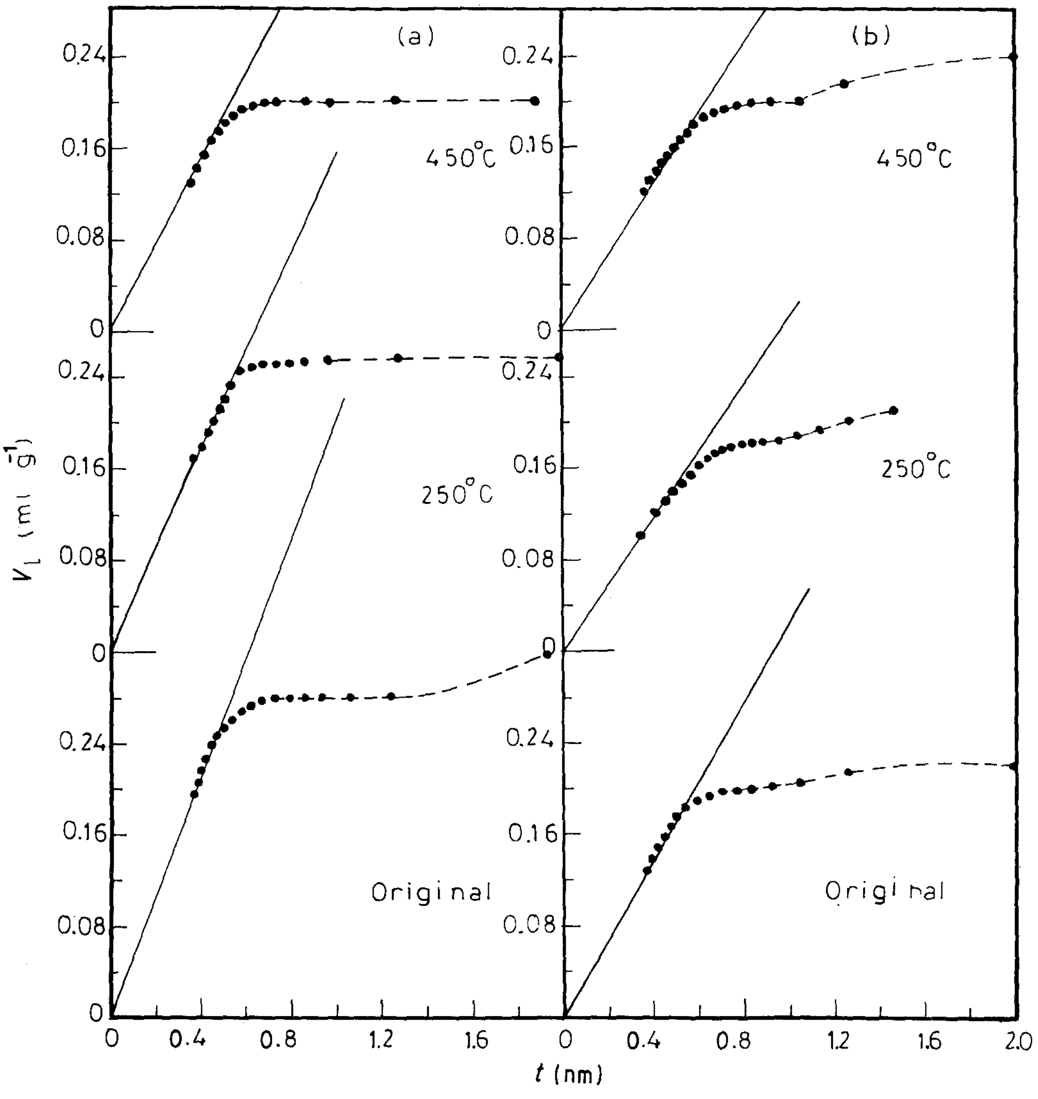

*Figure 8* $V_l$–$t$ plots of samples soaked for 2 days and their heated products: (a) series, I, (b) series II.

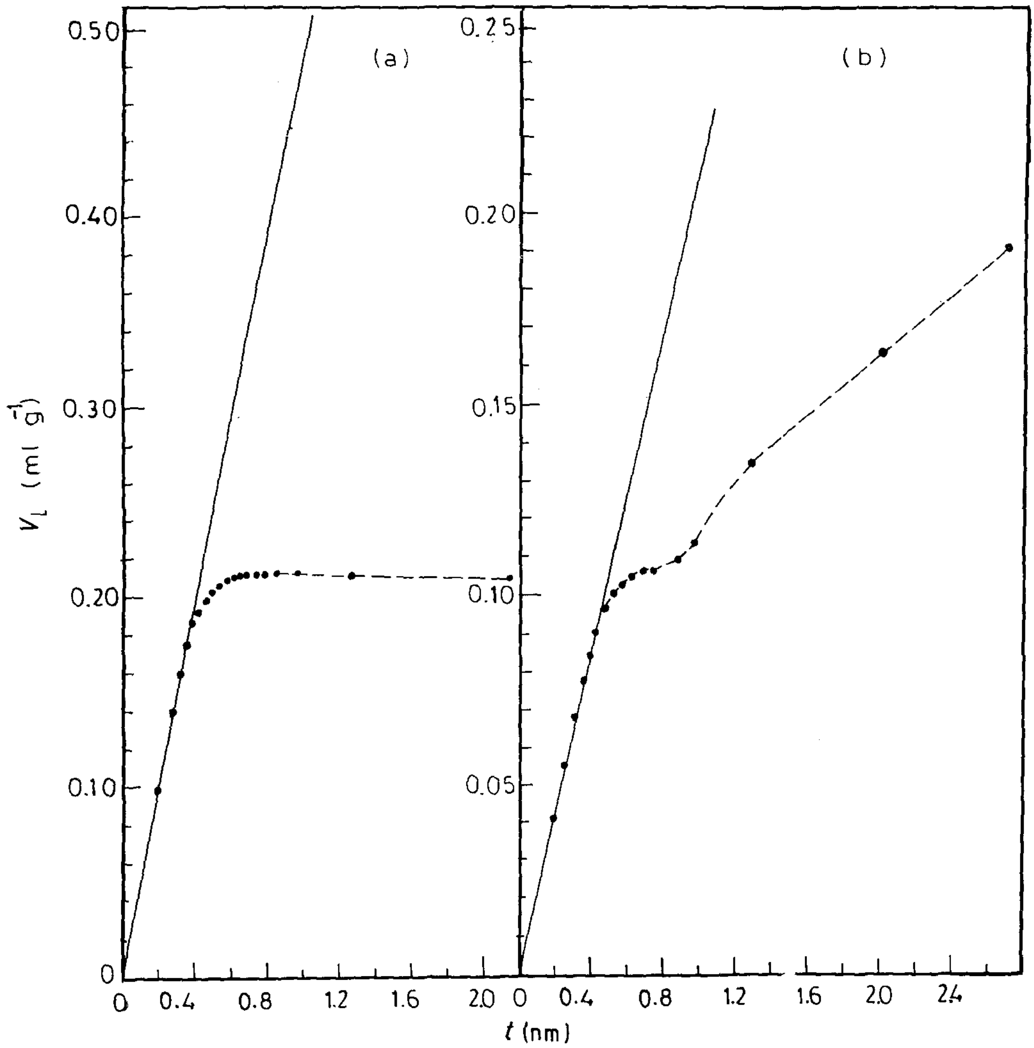

*Figure 9* $V_l$–$t$ plots of samples (a) $I_{5d}$ and (b) $II_{5d}$.

ward deviation, thus retaining the microporous texture of the support. However, for the samples from two groups of micropores could be distinguished that are well defined for the sample soaked for 7 days, where a clear step is observed at a $t$ value of ~ 0.48 nm. Maximum penetration seems to be achieved at this soaking condition that results in the appearance of these two groups of micropores. In these samples, the downward deviation exhibits a linear horizontal region up to a thickness of ~ 1.6 nm, above which a small upward deviation is observed as a result of interparticle condensation. However, for the sample soaked for 5 days, a marked increase in slope is observed commencing at a $t$ value of ~0.8 nm ($P/P_0$ ~ 0.75) pointing to increased adsorption in this region as a result of widening of a certain group of pores. This is also observed from the values of $r_H$ (assuming cylindrical pore idealization) where an increase to 1.40 nm is observed for this sample as well as a decrease in microporosity, $m_f$ (Table II, columns 6 and 7, respectively).

Heating to 250 °C results in the appearance of two groups of micropores for samples soaked for 5 h and 7 days commencing at a $t$ value of ~0.58 nm, with that of the latter soaking period exhibiting increased adsorption in the second group of pores ($t > 0.58$ nm). This is reflected in values of both $r_H$ and $m_f$. As to the sample soaked for 2 days, only one group of pores appeared with an average pore radius of ~1.20 nm. The presence of the two groups of micropores is no longer observed for samples heated at 450 °C except only slightly, for the sample soaked for 7 days. At this temperature, the double complex has already decomposed together with the evolution of any of water from the silica matrix.

As to samples of series II, a downward deviation is observed in the $V_l$–$t$ plots of all samples commencing at a $t$ value range of 0.4–0.48 nm depending on the pore dimension as compared to the $r_H$ values. Only one group of pores could be distinguished for all samples except that soaked for 7 days, where a small increase in slope is observed at a $t$ value > 0.58 nm ($P/P_0 > 0.50$). Heating to 250 °C causes some widening of the pores, especially for the sample soaked for 7 days where the downward deviation is shifted to higher $t$ values ( ~ 0.6 nm). In the case of the sample soaked for 5 h, a small initial upward deviation is observed that is not situated in the multimolecular adsorption region, signifying the occurrence of increased adsorption potential in this region of pore size ($P/P_0$ range 0.15–0.35). Widening of the pores at this temperature is also reflected in the values of $r_H$

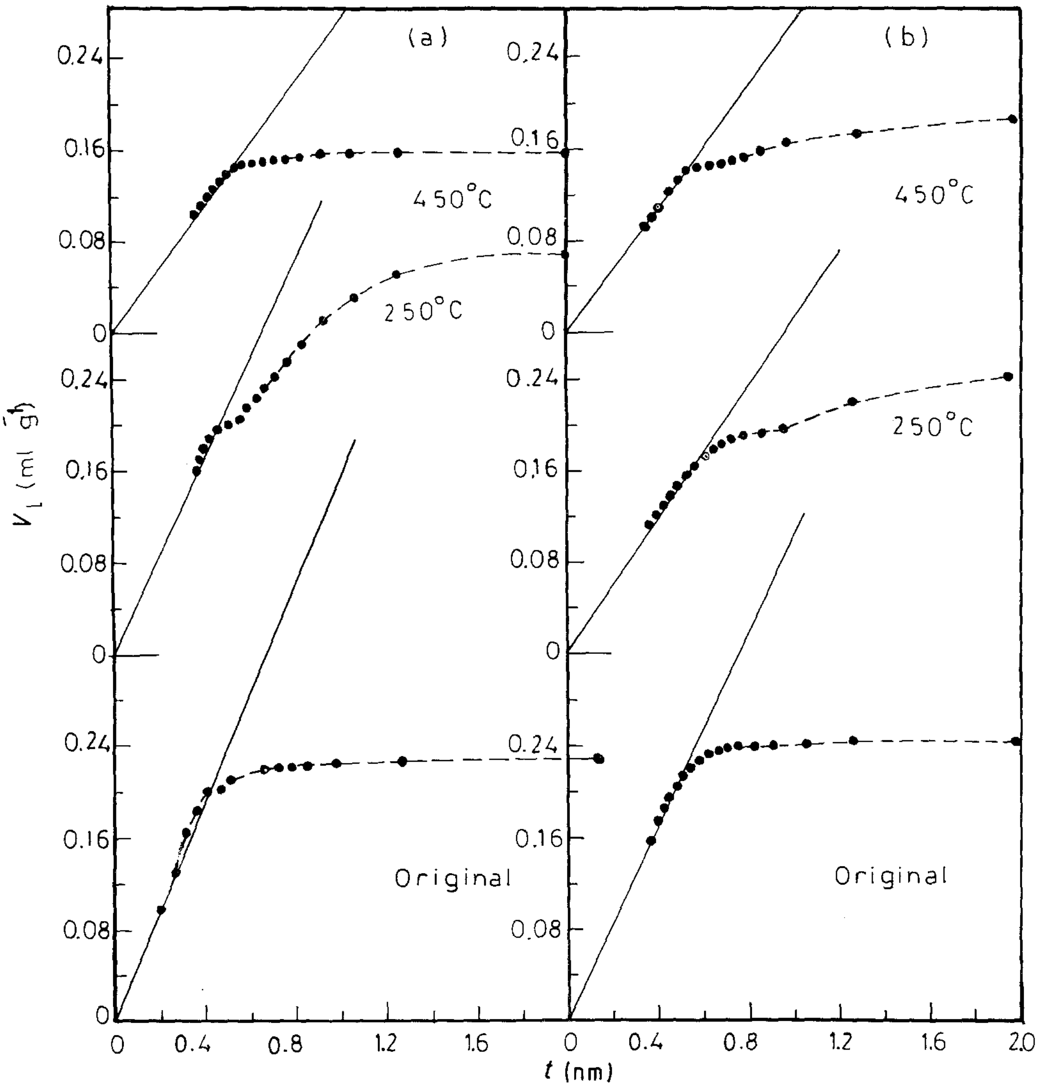

*Figure 10* $V_1$–$t$ plots of the samples soaked for 7 days and their heated products: (a) series I, (b) series II.

(Table III, column 6). At 450 °C, the predominancy of the microporous characteristics is still retained and the small increase in slope occurring in the $t$ value range 0.8–1.0 nm seems to result from pores between the particles, since it occurs at relative pressure $\geqslant 0.8$.

Thus, the textural characteristics observed for samples show clearly their dependence on the nature of the moiety used first in the precipitation of the double complex on the silica surface. It may depend not only on the texture of the support, but also on the chemistry of its surface that controls the sites available for each moiety type, whether cationic or anionic.

## References

1. J. GLERUP, *Acta Chem. Scand.* **26** (1972) 3775.
2. E. PEDERSON, *ibid.* **26** (1972) 333.
3. M. THOMSON and R. E. CONNICK, *Inorg. Chem.* **20** (1981) 2279.
4. A. EARNSHAW and J. LEWIS, *J. Chem. Soc.* (1961) 396.
5. R. A. de CASTELLO, C. P. MacCALL, N. B. EGEN and A. HAIM, *Inorg. Chem.* **8** (1969) 699.
6. J. E. HOUSE Jr and B. J. SMITH, *J. Inorg. Nucl. Chem.* **39** (1977) 777.
7. J. RAIBAS, J. CASABO, M. SERRA and J. M. CORONAS, *Inorg. Chem. Acta* **36** (1979) 41.
8. R. JEPSEN and J. E. HOUSE Jr, *J. Inorg. Nucl. Chem.* **43** (1981) 953.
9. A. HORVATH and M. MOHAI, *ibid.* **42** (1980) 195.
10. A. UEHARA, S. TERABE and R. TSUCHIYA, *Inorg. Chem.* **22** (1983) 2864.
11. S. KOHATA, M. ASAKAWA, T. MAEDA, H. SHYO and A. OHYOSHI, *Anal. Sci.* **2** (1986) 325.
12. J. R. ANDERSON, "Structure of Metallic Catalyst" (Academic, London, 1975) Ch.I.
13. J. BJERRUM and J. P. McRYNOLDS, *Inorg. Synth.* **2** (1966) 216.
14. J. V. SMITH (ed.), "X-ray Powder Data File and Index to X-ray Data File" (ASTM, Philadelphia, 1961).
15. ASM Powder Diffraction File, "Alphabetical Index of Inorganic Compounds" (International Center of Diffraction Data, Swarthmore, Pennsylvania, 1978).
16. F. A. COTTON and G. WILKINSON, "Basic Inorg Chem" (New Delhi, 1978) pp. 143–145.
17. P. K. GALLAGHER and C. R. KURKJIAN, *Inorg. Chem.* **5** (1966) 214.
18. L. KÉKEDY, A. SZUIKOS, R. KRÖBLE and E. KÉKEDY, *Acad. Rep. Populare Romine, Filiala Cliy* **9** (1958) 79.
19. C. DUVAL, *Anal. Chem. Acta* **16** (1957) 546.
20. K. NAKAMOTO, "Infra-red and Raman Spectra of Inorganic and Coordination Compounds" Pt. III (New York, 1977).
21. S. A. SELIM, S. HANAFI, M. ABD-EL-KHALIK and M. ISMAIL, *J. Chem. Tech. Biotechnol.* **35A** (1985) 297.
22. S. I. GREGG and K. S. W. SING (eds.), "Adsorption, Surface Area and Porosity" (Academic, London, 1967) Ch. 4.

23. M. G. KAGANER, *Zh. Fiz-Khim* **33** (1959) 2202.
24. B. C. LIPPENS, B. G. LINSEN and J. H. BOER, *J. Catal.* **3** (1964) 32.
25. J. H. de BOER, B. G. LINSEN and T. J. OSNIGA, *ibid.* **4** (1965) 643
26. B. C. LIPPENS and J. H. de BOER, *ibid.* **4** (1965) 319.
27. J. D. CARRUTHERS, P. A. GUTTING, R. E. DAY, M. R. HARRIS, S. A. MITCHELL and K. S. W. SING, *Chem. Ind.* (1968) 1772.
28. R. SH. MIKHAIL, N. M. GUINDY and S. HANAFI, *Egypt J. Chem., Special Issue Tourky* **53** (1973).

*Received 25 October 1990*
*and accepted 25 March 1991*